(Online) ISSN 2303-4521
Periodicals of Engineering and Natural Sciences *Original Research*
Vol. 13, No. 3, July 2025, pp.503-520

Quantitative assessment of the effects of climate change on water resources in the Huancané River basin, Peruvian Andes

Jhonatan Hinojosa-Mamani[1], Adderly Mamani-Flores[2*], Julian Apaza-Chino[3], Jorge Apaza-Ticona[4], Lucio Quea-Gutierrez[5], Naysha Sharon Villanueva-Alvaro[6], Alfredo Calderon-Torres[7], Vicente Alanoca-Arocutipa[8], Yuselino Maquera-Maquera[9], Sheylla Lía Cotrado-Lupo[10], Soledad Jackeline Zegarra-Ugarte [11], Juan Inquilla-Mamani [12]

[1] Department of Humanities, Faculty of Social Sciences, National University of the Altiplano, Puno, Peru
[2] Department of Anthropology, Faculty of Social Sciences, National University of the Altiplano, Puno, Peru
[3] Department of Mines, National University of the Altiplano, Puno, Peru
[4] Department of Anthropology, Faculty of Social Sciences, National University of the Altiplano, Puno, Peru
[5] Department of Mines, National University of the Altiplano, Puno, Peru
[6] Department of Dentistry, National University of the Altiplano, Puno, Peru
[7] Department of Anthropology, Faculty of Social Sciences, National University of the Altiplano, Puno, Peru
[8] Department of Anthropology, Faculty of Social Sciences, National University of the Altiplano, Puno, Peru
[9] Department of Social Work, National University of the Altiplano, Puno, Peru
[10] Department of Accounting, Faculty of Social Sciences, Andean University of Cusco, Peru
[11] Department of Social Work, National University of the Altiplano, Puno, Peru
[12] Department of Sociology, Faculty of Social Sciences, National University of the Altiplano, Puno, Peru

*Corresponding author E-mail: adderlymamani@unap.edu.pe

ABSTRACT

The purpose of this article is to evaluate the effects of climate change on surface runoff, aquifer recharge, percolation and renewable water resources in the Huancané River basin, Puno – Peru, using the SWAT hydrological model and the standardized precipitation index (SPI). The RCP 4.5, RCP 8.5, SSP1-2.6 and SSP3-7.0 climate scenarios of CMIP5 and CMIP6 were applied for the projected period 2025–2100. The model was calibrated and validated with historical data from the period 1981–2016. The results showed that surface runoff will decrease significantly in the most extreme scenarios, reaching only 8.09 m³/s in SSP3-7.0, while in RCP 8.5 a maximum of 12.59 m³/s is projected. The recharge of the aquifer will be reduced from 559.22 Mm³ to 179.09 Mm³ and the volume of renewable water will decrease by 51.2%, from 750 Mm³ to 366 Mm³. In addition, the average annual temperature in the basin could reach 14°C by the end of the 21st century, increasing evapotranspiration and further reducing water availability. The SPI index projects an intensification of droughts during the period 2025–2050. These scenarios show a growing vulnerability of the water system, which represents a critical challenge for agriculture, supply and sustainability. The integration of the SWAT model with climate projections is a key tool for water planning and adaptation in vulnerable Andean regions.

Keywords: Climate change, SWAT Modeling, CMIP6 Scenarios, Droughts, Tropical Andes.

1. Introduction

The effects of climate change are very salient and its importance of processes, including the hydrological cycles of environmental conditions and the ecological balance of ecosystems and the management and planning of water resources, are complicated due to the consequences of climate change uncertainties[1], [2], which represents a major concern due to the increase in temperature worldwide and variations in rainfall patterns and extreme weather events that change the total and seasonal water supply [3],[4]. In this context, the floods in the Andean basin of Huancané are strongly related to the level of Lake Titicaca, for example, two heavy floods were recorded between 1982 and 1986, and 2003 and 2004 [5],[6]. Over time, scenarios have been developed to estimate the effects of rising greenhouse gases on global temperature. RCPs represent different levels of radioactive forcing and help assess future climate uncertainty in variables such as temperature and precipitation. More recently, the IPCC introduced SSPs, which incorporate socioeconomic factors that influence emissions and adaptation to climate change. The combination of RCP and SSP allows for a comprehensive analysis of

future climate impact. According to projections, the temperature will continue to rise in all scenarios, and exceed 1.5°C or 2°C [7], [8]. In this context, it is important to use the SWAT hydrological model to simulate the water cycle and water availability under different climate and land use scenarios [9], [10]. Consequently, SWAT is a physically-based model capable of simulating the spatial and temporal distribution of water resources, making it an especially useful tool for areas with limited observational data. In Peru, the incorporation of gridded climate databases, such as RAIN4PE (Rain for Peru and Ecuador) and PISCO (Peruvian Interpolated data), which provide high-resolution precipitation data from both satellite and terrestrial sources, improves the accuracy of hydrological models and enables more reliable projections in areas with limited information [11], [12].

Precipitation and temperature data applied the CMhyd and SWAT models to study climate change-related runoff and sediment uncertainty in future periods of 2015 and 2100 under Global Circulation Models (GCMs) [13]. The Standardized Precipitation Index (SPI) was designed to identify and monitor droughts, taking into account precipitation alone as a variable to determine the presence of a rainfall deficit or surplus in a specific region during a given period under normal conditions [14],[16]. It is one of the most widely used indices in Europe to monitor different types of droughts [17], [18]. The SWAT model has been used to assess the impacts of climate change in the Budhigandaki River Basin, projecting an increase in annual flows and greater variability at extremes under RCP4.5 and RCP8.5, highlighting the need for adaptation in water management [19]. According to Daneshvar et al. (2021) they used SWAT that was adapted for southern Peru with local and satellite data, showing reliable predictions. The basin is dominated by baseflow, with less than 9% of surface runoff and 62% of precipitation lost to evapotranspiration. These methods are useful for watersheds with limited data in the Peruvian Andes. This study evaluates the management of water resources in Arequipa, using climate change models and socioeconomic scenarios. An increase in flows is projected during the wet season, with increases of up to 704% in reservoir inflows. Although water deficits are not expected, improved storage and irrigation efficiency is required to avoid losses during the wet season[20]. The research evaluates the impact of land-use change (LULC) on the water balance of the Puyango-Tumbes basin (Ecuador and Peru) between 1981 and 2015. An increase of 18.3% was detected in grasslands and a reduction of 38.2% in savannahs, which increased Evapotranspiration (PET) by 2.1% and reduced Percolation (PERC) by 29.2%, Runoff (SURQ) by 20.7% and Groundwater Flow (GW_Q) by 33%. These changes highlight the importance of properly managing water resources [21]. On the other hand, Xiaolu et al. (2021) this analysis used SWAT to assess the impact of irrigation in Majes, Arequipa, with 49 sub-basins and 4222 HRUs. Agricultural infiltration affects the groundwater flow and the Siguas River. Climate variability impacted surface runoff more (70%) than groundwater flow (30%). It is recommended to monitor sustainable water management in the face of climate change [22].

Given the different climate changes around the world, Peru cannot be excluded from these large-scale changes, the consequences of which are observed in many Peruvian basins, as has been seen, very few studies have evaluated the effects of climate change on water resources. The purpose of this study is to analyze the impact of climate change on renewable water resources in the Huancané River basin, through hydrological simulations with the SWAT model and climate projections derived from the MPI_ESM_MR and ACCESS1_0 models (RCP 4.5 and 8.5), as well as MPI-ESM1_2_HR and ACCESS_CM2 (SSP1-2.6 and SSP3-7.0). on the horizon 2025–2100. The aim is to estimate the projected variations in runoff, groundwater recharge and percolation, to guide decision-making in water management

1.1. Theoretical framework

1.1.1. Climate change and hydrological systems

Climate change represents one of the most significant global challenges, with profound implications for hydrological cycles (IPCC, 2021). Rising temperatures, altered precipitation patterns, and increased frequency of extreme weather events directly influence the availability, distribution, and quality of water resources [23]. These changes can disrupt the seasonal flow regimes, alter snowmelt dynamics, and increase evapotranspiration, especially in high mountain ecosystems like the Andes [24].

The Andean basins, including those in Peru, are characterized by complex topography, climate variability, and a dependence on glacial and rainfall contributions for streamflow [25]. In regions such as Huancané, river discharge is influenced by both precipitation and glacier meltwater. These hydrological dynamics are sensitive to even minor climatic fluctuations, making them critical indicators of climate change impacts [26].

The Peruvian Andes have experienced significant glacier retreat over the past decades due to increasing temperatures, affecting water availability for agricultural, domestic, and ecological uses [27]. Basins like Huancané are particularly vulnerable due to their reliance on seasonal water inputs and limited water storage

infrastructure. Understanding the temporal variability and future trends in streamflow is essential for sustainable water management in these regions [25].

1.1.2. Quantitative modeling and climate projections

Hydrological modeling, supported by quantitative methods and climate scenarios (e.g., RCP 4.5, RCP 8.5), allows for the simulation of water resource responses to different climate futures [28]. Models such as SWAT (Soil and Water Assessment Tool) and WEAP (Water Evaluation And Planning) are widely applied in Andean contexts to evaluate changes in runoff, infiltration, and evapotranspiration under varying climatic inputs [29]. The use of downscaled General Circulation Models (GCMs) further enhances the accuracy of regional assessments.

Studies in the southern Peruvian Andes have documented the reduction of glacial-fed water flows and shifts in seasonal hydrological patterns [30]. In the neighboring basins of Lake Titicaca, researchers have observed a correlation between decreasing precipitation and reduced surface water flows, emphasizing the urgent need for local adaptation strategies [31]. These findings underscore the importance of site-specific assessments, such as the one proposed for the Huancané basin.

Despite the growing body of literature on climate impacts in Andean basins, there remains a lack of detailed quantitative analyses at the sub-basin scale, particularly in the Huancané River basin. This research addresses this gap by integrating climate projections and hydrological modeling to assess the current and future water availability, offering valuable insights for policy-making, community planning, and climate resilience strategies.

2. Research method

2.1. Study area

This study was carried out in the basin of the Huancané River covers an approximate area of 3,522 km², with a maximum altitude of 5,162 meters above sea level in the South Puna hill and a minimum of 3,812 meters above sea level at its mouth in Lake Titicaca. Geographically, it extends between latitudes 14.3° and 15.6° south, and longitudes 69.2° and 70.4° west, as illustrated in the corresponding figure. Figure 1.

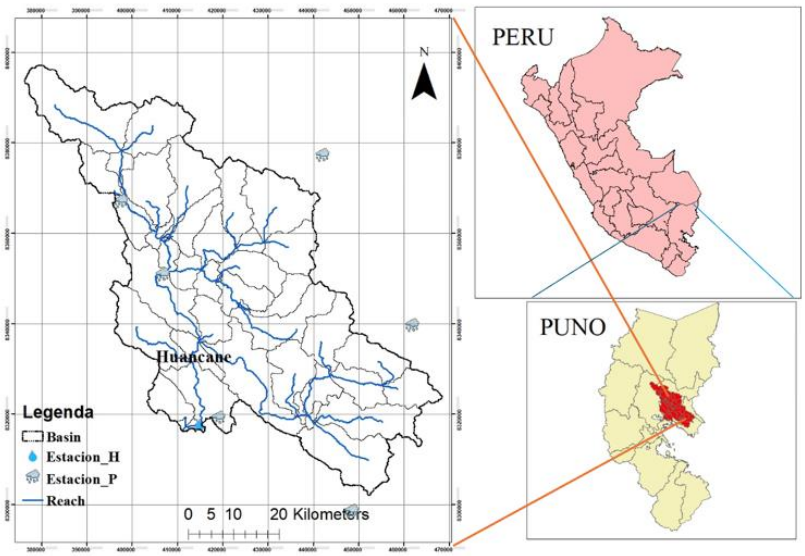

Figure 1. Study Basin and Stations

The Huancané River basin is formed at the confluence of the Quellocarca and Tuyto rivers, and from this point it acquires its name to its mouth in Lake Titicaca. Its main course extends approximately 125 km from its sources to the lake. Before its arrival in it, there is the Puente Huancané hydrometric station, managed by SENAMHI and data PISCO V2.1 gridded[32], where the flows contributed by the river are monitored. Access to the study area from the city of Puno is through the paved road Puno – Juliaca – Huancané, with an approximate distance of 92 km. As for its limits, the Huancané River basin is bordered to the east by the Suches and Huaycho river basins, to the west by the Azángaro River basin and the Ramis inter-basin, to the north by the Azángaro River basin and to the south by Lake Titicaca.

2.2. SWAT database

In this study, the SWAT hydrologic model [33] It was developed using spatial and climatic information from various sources. A DEM (Digital Elevation Model) layer with a resolution of 90 m was used, obtained from the Alaska Satellite Facility (ASF), which allowed the delineation of the basin and the definition of the hydrographic network in the ArcGIS environment. In addition, a soil layer at a resolution of 1:5 000 000 from FAO (1995 and 2003), and a vegetation cover layer with a spatial resolution of 300 m, provided by the USGS through the Earth Explorer portal, were used.In the first phase of modeling, the Huancané River basin was divided into 42 sub-basins based on topography and the network of dividing lines. Subsequently, each sub-basin was fragmented into a total of 1,649 Hydrological Response Units (HRUs). Figure 2. defined by unique combinations of land use, soil type, and slope. This procedure allowed a detailed and spatially explicit representation of hydrological processes throughout the basin.

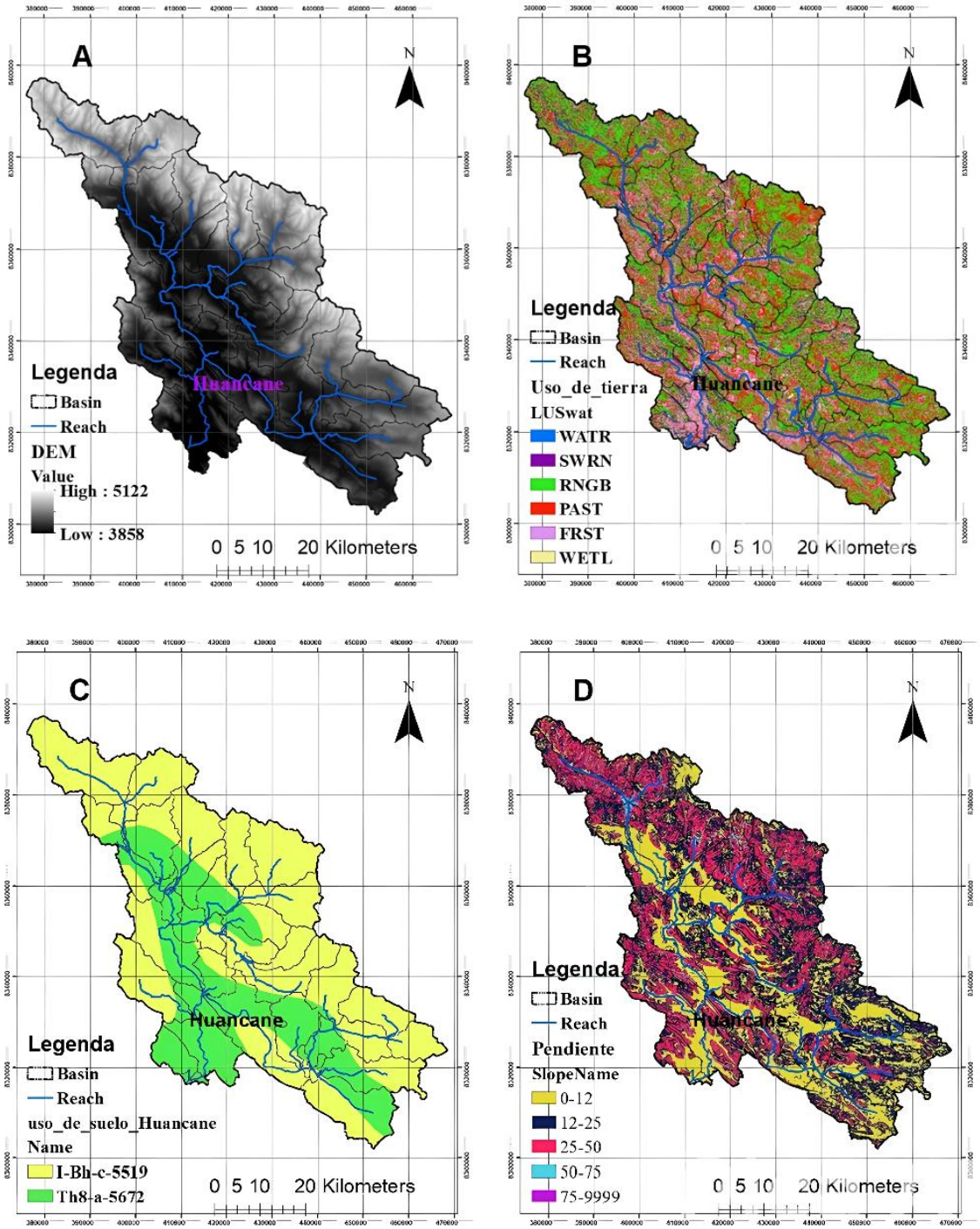

Figure 2. Digital Elevation Model (DEM) (A), Land Use (B), Soil Map (C), Soil Slopes (D)

The daily records of minimum temperature, maximum temperature and precipitation from six meteorological stations were incorporated into the model, in order to simulate the hydrological processes corresponding to the period 1981–2024, using the SWAT model (version 2012) in the ArcGIS 10.8.26 software environment. The calibration and validation of the model was carried out using the monthly flows observed in a hydrometric station, applying the SWAT-CUP software using the SUFI-2 algorithm. The technical specifications of the Puente Huancané hydrometric station are detailed in Table 1.

Table 1. Characteristics of the Latin Hydrometric Station

Season	Station code	Height	Longitude	Latitude
Huancané Bridge	210201	3821	69°47'33.4'	15°12'57.2''

2.3. Annual climate scenarios generated using GCM

Global Climate Models (GCMs) are fundamental tools for assessing the impacts of climate change and simulating the responses of the climate system to different trajectories of greenhouse gas concentration.[34], [35].

In the present study, climate data generated by four models were used four different models were downloaded in the SSP1-2.6 and SSP3-7.0 scenarios The CMhyd model was used for bias correction of projected precipitation and temperature estimates based on GCM at the basin scale [36], [37]. successfully overcome the bias between observed and simulated climate variables based on GCM indicators in various regions of the world[38]. GCMs corresponding to the CMIP5 and CMIP6 projects: ACCESS1-0 and MPI-ESM-MR of CMIP5, and ACCESS-CM2 and MPI-ESM1-2-HR of CMIP6. These models were selected for their robustness in simulating regional climatic conditions and their compatibility with hydrological modeling tools. The climate simulations were developed under four representative concentration scenarios: RCP 4.5 and RCP 8.5 of CMIP5, as well as SSP1-2.6 and SSP3-7.0 of CMIP6. To ensure the hydrological applicability of the projections, the CMhyd model was used with the aim of performing spatial disaggregation, data extraction, downscaling and bias correction of the gross climate outputs of the GCMs. In this way, a set of adjusted daily climate data was obtained that were used as input in the SWAT hydrological model, allowing a comparative analysis of the trends in temperature, precipitation and other climate variables under different emission trajectories for the period 2025–2100.

CMIP6 introduces substantial advances over CMIP5, including higher spatial and temporal resolution, improved representation of physical processes such as aerosol-cloud interactions, and more accurate simulation of extreme events. Unlike CMIP5, which relied on Representative Concentration Pathways (RCPs), CMIP6 uses Shared Socioeconomic Pathways (SSPs), integrating socioeconomic factors with emissions to provide more realistic and policy-relevant scenarios. Additionally, many CMIP6 models exhibit higher climate sensitivity, implying greater projected temperature increases and, consequently, a potential intensification of hydrological impacts. These differences make CMIP6 more suitable for detailed regional climate change assessments, such as those conducted in the Huancané River basin.

Table 2. A summary of the characteristics of the Special Report on Emission Scenarios (ESRES) on climate scenarios (A1, A2, B1 and B2) in 2100 compared to 1990.

Stage Feature	1990	RCP 4.5	RCP 8.5	SSP1-2.6	SSP3-7.0
World Population (Billion)	525	9.3	12.0	8.5	11.2
CO_2 in the Atmosphere (ppm)	354	538	936	421	821
World Economic Growth Index	2	600	800	900	300

2.4. Running the SWAT model

SWAT is a continuous hydrological model oriented at the basin scale, developed to evaluate the effects of various management strategies on water, sediment and agrochemical levels in large and complex watersheds, which exhibit variability in soils, land uses, morphological conditions and long-term management practices [33], [39], [40]. It is a physical model of spatial distribution that allows the analysis of problems related to soil

and water. Unlike empirical models based on regression equations, SWAT operates using observational data of climate, soil properties, topography, vegetation cover, land use, and management practices implemented in the watershed the scheme shown. Figure 3, SWAT is a distributed model that divides a basin into sub-basins and discretizes them into Hydrologic Response Units (HRUs). The initial configuration includes watershed delineation and the use of slope, land use, and soil data to define the HRUs. This approach assumes that lands with similar characteristics show similar hydrological behaviors[41], [42]. From this data, it indirectly simulates physical processes such as water flow, sediment transport, plant growth, and nutrient cycling using defined input parameters. It is a computationally efficient model, designed to simulate large-scale, high-complexity watersheds with a low processing cost, thus enabling the analysis of prolonged impacts such as erosion, diffuse pollution, and sedimentation. The operation of the model is based on a comprehensive database that determines the values and limits of the parameters for each component, including the location and data of meteorological and climatic stations, as well as the current agricultural and water management practices of the study area. Inputs to the model are generally organized into point and spatial data.

In this study, the SWAT hydrologic model was used to evaluate water management strategies at the basin level. SWAT is a physically-based hydrological simulation tool with a semi-distributed approach that allows hydrological processes to be represented in differentiated geographical spaces. It uses the Soil Conservation Service (SCS) method to estimate runoff, and simulates phenomena such as surface runoff, snow melt, lateral flow, and underground drainage. It also allows the calculation of the water balance and flow in rivers, based on one (1) fundamental that integrates water inputs, outputs and storage. The SWAT hydrologic model is based on the basic equation of the water balance:

$$SW_t = SW_0 + \sum_{t=1}^{t} (R_d - Q_s - E_a - W_{seep} - Q_{gw}) \quad (1)$$

Where denotes the total water content in the soil, it is the initial soil moisture level, and represents the time expressed in days. is the daily precipitation, while it refers to the surface runoff generated. It is the actual evapotranspiration, it is the volume of water that infiltrates into the unsaturated zone (vadose) during the day, and indicates the return flow or underground runoff that occurs that same day.$SW_t SW_0 t R_d Q_s E_a W_{seep} t Q_{gw} t$

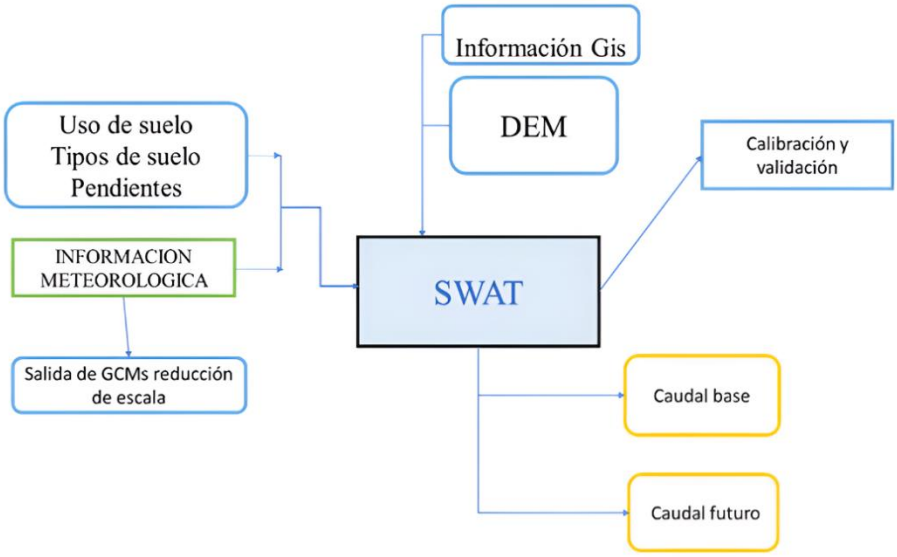

Figure 3. Model flowchart illustrating the integration of the Soil and Water Assessment Tool (SWAT) models

2.5. Calibration analysis

Due to the large number of parameters present in the SWAT model and the simultaneous simulation of various hydrological and agricultural variables, it was performed using the SWATats Calibration and Uncertainty Procedures (SWAT-CUP) software [43] in which a sensitivity analysis and subsequent calibration were carried out. There are two approaches to sensitivity analysis: a local one, which can be related to time, and a global one.

In local sensitivity analysis, a single parameter is adjusted within a predefined range while the others remain constant, thus evaluating changes in the model results based on the variation of each parameter. A parameter that has a higher absolute value in the t-stat and a p-value close to zero will have a more significant impact on the variable analysed[44], [45]. The calibration of the model was performed using the coefficient of determination (R^2) and the Nash-Sutcliffe coefficient of efficiency (NS).

2.6. Standard precipitation index (SPI)

This index was first proposed in 1993 by McKee et al. and is calculated for each region considering the historical record of its rainfall. It is one of the simplest and most widely used drought indices, as it compares normalized rainfall with average rainfall to show the deficit or excess of rainfall in a specific period of time, location, and climate [46], the SPI is supported globally by the World Meteorological Organization (WMO) for drought assessment [47]. For the evaluation of droughts using the SPI index, precipitation is the only data required. Initially, an appropriate statistical distribution is adjusted to the long-term rainfall data[22]. Subsequently, the cumulative distribution function is transformed into a normal distribution using equivalent probabilities, according to (2).

$$SPI = \frac{X_i - X^-}{S_n} \tag{2}$$

$X^-$is the average precipitation per month, Sn is the standard deviation on the time scale, and is the rainfall per month. X_i

Due to the normality of the SPI Index, dry and wet climates can also be monitored using the SPI Index. Table 3 lists the drought classification based on the SPI index

Table 3. Drought Classification

SPI Values	
$SPI \geq 2.0$	Extremely humid
$1.5 \leq SPI < 2.0$	Very humid
$1.0 \leq SPI < 1.5$	Moderately humid
$-1.0 < SPI < 1.0$	Close to normal
$-1.0 \geq SPI > -1.5$	Moderately dry
$-1.5 \geq SPI > -2.0$	Severely with him
$-2.0 \geq SPI$	Extremely dry

The analysis of drought conditions using the Standardized Precipitation Index (SPI) reveals an increasing frequency and intensity of meteorological droughts in the Huancané River basin, particularly under high-emission scenarios. These SPI-based drought classifications are closely linked to hydrological impacts such as reduced streamflow, lower groundwater recharge, and diminished water availability during the dry season. The correspondence between negative SPI values and periods of decreased river discharge highlights the basin's sensitivity to precipitation deficits. This connection underscores the utility of the SPI as an early indicator of hydrological stress, reinforcing the need for integrated drought monitoring and adaptive water management strategies in the context of climate change.

3. Results and discussion

3.1. Analysis of the variability of model parameters

The period between 1981 and 2024 was selected after a statistical analysis of data from climatological and hydrometric stations in the basin studied, also considering the objectives of the research and the need to have inputs modeled in continuous and simultaneous time series. Within this interval, the years 1981-2016 were used for the calibration phase, while the last three years (2017-2024) were used for model validation. To carry out the calibration and validation of the SWAT model, monthly time series of the observed data were prepared,

using the SWAT-CUP software together with the SUFI-2 algorithm. In total, 103 key parameters were adjusted and validated for the simulation of runoff in the model.

The parameters with the greatest impact on the flow are presented in Table 4. As for the codes used, the letter V indicates the replacement of a parameter with a new value, while the letter R represents the multiplication of the original parameter by (1 + a certain value), thus replacing the initial parameter. On the other hand, Table 3 shows the effects of various relevant parameters in the simulation of the flow in the sub-basins, accompanied by their respective p-values and t-stats. Those parameters with a higher absolute t-stat value and a p-value close to zero exerted a greater influence on the flow of the current.

Table 4. Sensitivity analysis and determination of the effective parameters of the model; V: Replacing a parameter value with a new value of a new parameter; R: parameter value multiplied by (1 + given value)

Parameter Code	Description	T -stat	P-Value
v__CH_N2.rte	Curve number	0.88	0.47
v__ESCO.game	Soil evaporation compensation factor	-0.23	0.84
v__GW_REVAP.gw	Groundwater re-evaporation coefficient	0.27	0.81
v__REVAPMN.gw	Threshold depth of water in the shallow aquifer for re-evaporation to occur (mm)	0.30	0.80
v__GWQMN.gw	Threshold of water depth in the shallow aquifer required for the return flow to occur (mm)	0.76	0.53
v__GW_DELAY.gw	Groundwater delay (days)	0.61	0.61
v__ALPHA_BF.gw	Baseflow Recession Constant	0.38	0.74
v__RCHRG_DP.gw	Percolation fraction of deep aquifers	-0.08	0.94
v__CH_K2.rte	Effective hydraulic conductivity in main channel alluvium (mm h^{-1})	0.69	0.56
v__TIMP.bsn	Snow cover temperature lag factor	-0.26	0.82
v__SURLAG.bsn	Coefficient of delay of surface runoff (day)	0.01	1.00
v__SFTMP.bsn	Base snow melt temperature (°C)	-0.24	0.83
v__SMTMP.bsn	Snowfall temperature (°C)	0.45	0.70
v__SMFMX.bsn	Maximum melt factor for June 21 (mm H_2O $°C^{-1}$ day^{-1})	0.64	0.59
v__SMFMN.bsn	Minimum melt factor for December 21 (mm H_2O $°C^{-1}$ day^{-1})	-0.05	0.97

3.2. Model calibration and validation

After performing the sensitivity analysis, the calibration and validation of the model was carried out using monthly data from Latin American hydrometric stations. The simulations were evaluated using the coefficient of determination (R^2) and the Nash-Sutcliffe coefficient of efficiency (NS), as detailed in Table 5. As can be seen in Figure 4, despite the large size of the basin, the final results of the calibration reflect the ability of the SWAT model to accurately represent the hydrological behavior of the basin.

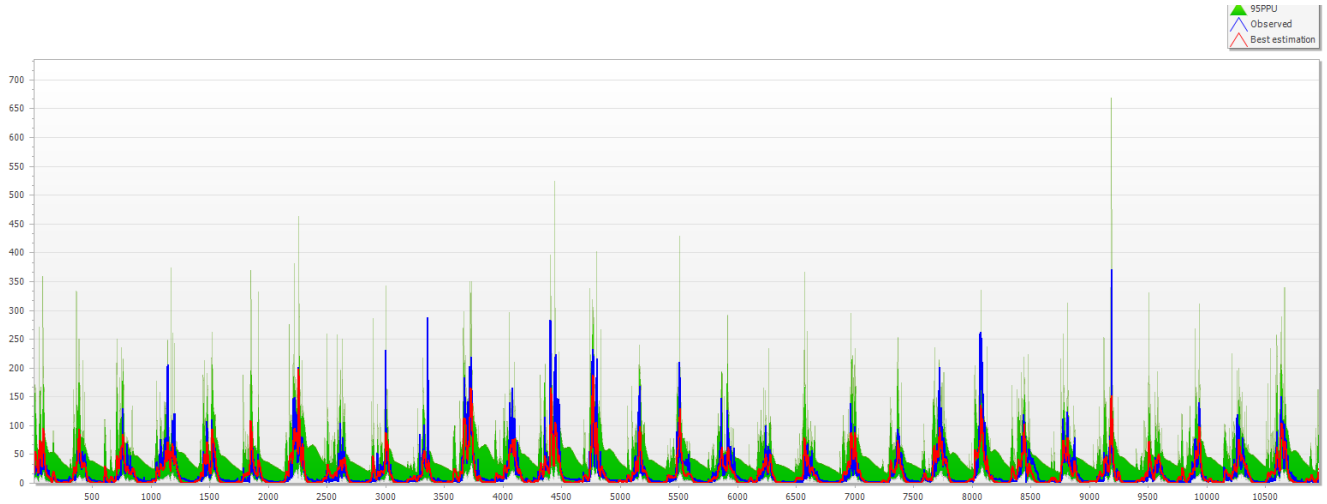

Figure 4 Graph of observed and simulated time series with 95% probability band (Latiana hydrometric station)

Table 5. Calibration and validation results for each hydrometric station in the period 1981–2016. R2: coefficient of determination; NS: Nash–Sutcliffe coeffcient

Season	Rio	Station code	R^2	NS	R^2	NS
			Calibration		Validation	
Huancané Bridge	Huancané	2102001	0.75	0.73	0.85	0.81

3.3. Annual runoff simulation

Since the SWAT model simultaneously requires temperature and precipitation data, multiple climate models from the CMIP5 and CMIP6 sets were selected to assess the future hydrological behavior of the Huancané River basin. In this case, the MPI-ESM-MR and ACCESS1_0 models for CMIP5 under the RCP 4.5 and RCP 8.5 scenarios were considered, and the MPI-ESM1-2-HR and ACCESS-CM2 models for CMIP6 under the SSP1-2.6 and SSP3-7.0 scenarios. Time series of meteorological data corrected by statistical methods were generated and integrated into the SWAT model to simulate runoff in the period 2025–2100.The results obtained reveal that, compared to the historical value of annual average runoff (4.59 m³/s), the RCP scenarios project significant increases, with values greater than 12 m³/s under RCP 8.5 in the ACCESS1_0 model (12.59 m³/s) and RCP 8.5 in MPI-ESM-MR (12.28 m³/s). However, the simulations under the CMIP6 framework present more moderate values. In particular, the SSP1-2.6 and SSP3-7.0 scenarios project gradual reductions towards the end of the century, reaching 9.43 m³/s and 8.09 m³/s respectively, the latter being the lowest value projected among all models. Figure 5

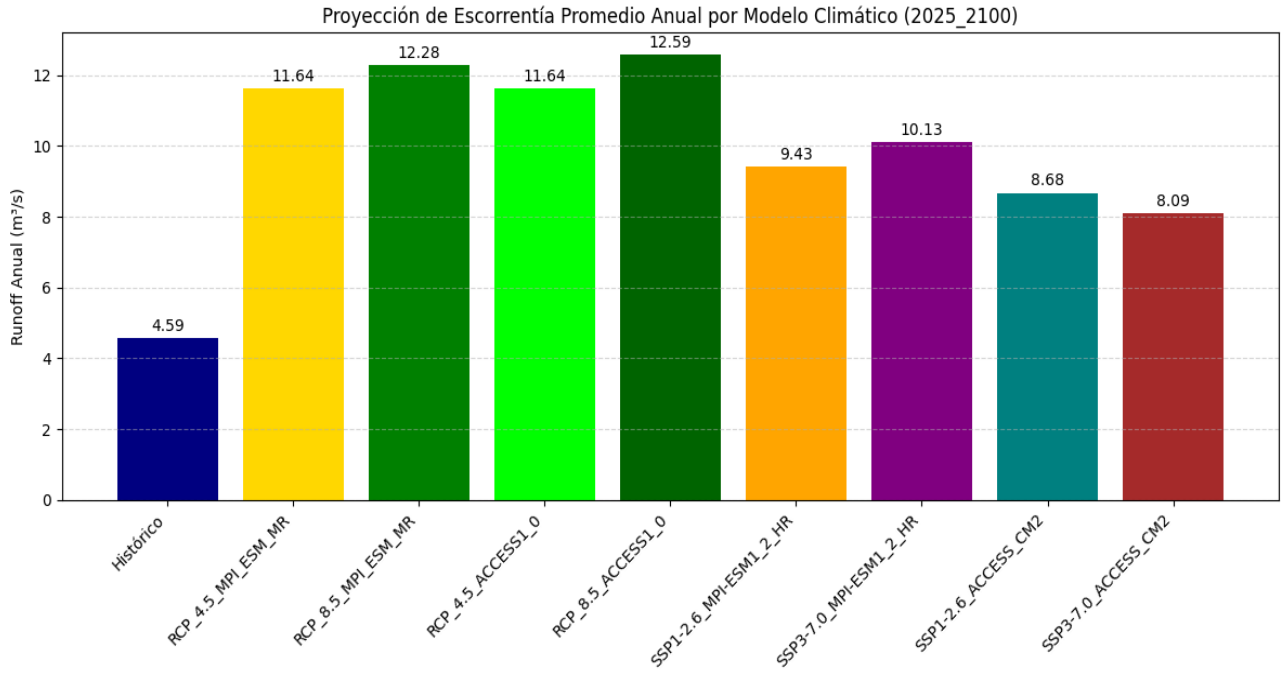

Figure 5. Simulation of runoff under the climate scenarios examined.

These projections are strongly influenced by changes in temperature and precipitation. According to climate simulations, the average annual temperature in the Huancané basin will increase progressively, reaching up to 14 °C in the SSP3-7.0 – MPI ESM1 2 HR scenario towards the end of the century, while annual precipitation, although with great interannual variability, shows a slightly decreasing trend in several scenarios, especially in the SSP1-2.6 – ACCESS CM2 Table 5. This combination of higher temperature and lower precipitation generates conditions more prone to a decrease in surface runoff and water availability. Therefore, the models indicate that, although some scenarios could show temporary increases in runoff, towards the end of the century the water balance will tend to reduce. This could negatively affect the sustainability of water use for agricultural, domestic and ecosystem activities in the Huancané basin.

Table 6. Simulation of runoff and surface water under the climate scenarios examined.

Model	Scenario	Period	Water surface (Mm^3)	Runoff ($m^{3/s}$)
	Base		144.88	4.59
MPI_ESM_MR	RCP 4.5	2025–2100	367.16	11.64
MPI_ESM_MR	RCP 8.5	2025–2100	387.36	12.28
ACCESS1_0	RCP 4.5	2025–2100	367.16	11.64
ACCESS1_0	RCP 8.5	2025–2100	396.93	12.59
MPI-ESM1_2_HR	SSP1-2.6	2025–2100	297.46	9.43
MPI-ESM1_2_HR	SSP3-7.0	2025–2100	319.33	10.13
ACCESS_CM2	SSP1-2.6	2025–2100	273.78	8.68
ACCESS_CM2	SSP3-7.0	2025–2100	255.28	8.09

3.4. Simulation of percolation dynamics in the aquifer

After evaluating the ability of climate models to simulate runoff, the behavior of percolation and groundwater recharge in the basin under historical conditions and future scenarios was analyzed. During the base period (1981–2016), groundwater recharge reached 559.22 Mm³ and estimated discharge was 335.53 Mm³ Table 7, values significantly higher than those projected in all climate scenarios for the period 2025–2100. The RCP_4.5_MPI_ESM_MR and RCP_8.5_MPI_ESM_MR models show a substantial decrease, with recharges of 231.63 Mm³ and 179.09 Mm³ respectively, while their estimated discharges stand at 138.98 Mm³ and 107.46 Mm³. In contrast, the SSP scenarios show slightly higher values: for example, the SSP_2_6_MPI_ESM1_2_HR model projects a recharge of 259.36 Mm³ and a discharge of 155.69 Mm³. These reductions in groundwater recharge and discharge are associated with the decrease in projected precipitation, as observed in the climate change figures, as well as the sustained increase in annual temperature, which intensifies evapotranspiration and limits infiltration. The scenario with the greatest impact is the RCP_8.5_MPI_ESM_MR, which represents a context of high emissions and greater climate variability, with a total recharge of less than 180 Mm³.

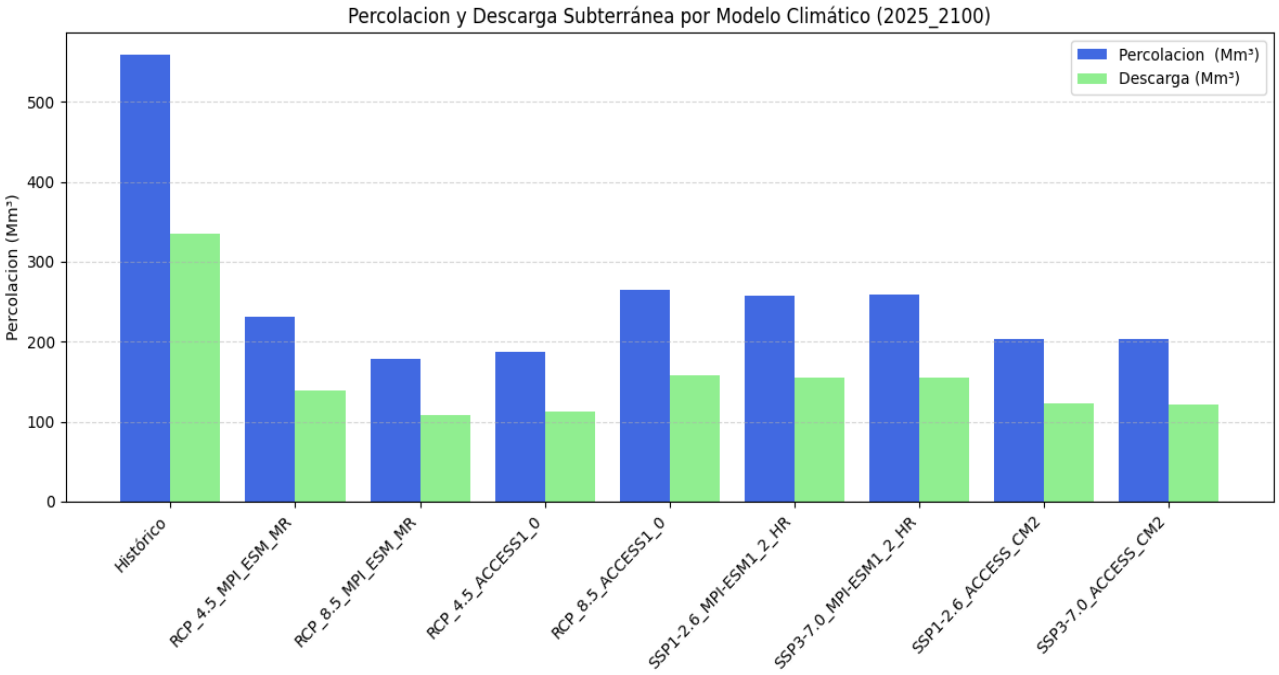

Figure 6. Simulation of aquifer percolation under the climate scenarios examined.

Overall, the combination of lower precipitation and projected thermal increase compromises groundwater availability for the coming years, posing a major challenge for sustainable resource management.

Table 7. The simulation of aquifer percolation under the climate scenarios examined.

Model	Scenario	Period	Groundwater Recharge(Mm^3)	Discharge (Mm^3)
Base			559.22	335.53
MPI_ESM_MR	RCP 4.5	2025–2100	231.63	138.98
MPI_ESM_MR	RCP 8.5	2025–2100	179.09	107.46
ACCESS1_0	RCP 4.5	2025–2100	186.64	111.99
ACCESS1_0	RCP 8.5	2025–2100	264.28	158.57
MPI-ESM1_2_HR	SSP1-2.6	2025–2100	257.26	154.36
MPI-ESM1_2_HR	SSP3-7.0	2025–2100	259.21	155.53
ACCESS_CM2	SSP1-2.6	2025–2100	203.98	122.39
ACCESS_CM2	SSP3-7.0	2025–2100	203.27	121.96

3.5. Modeling of renewable water resources

Based on data obtained from the SWAT model and synthesized in the Comparative Figure, it is evident that the volume of renewable water will decrease markedly towards the end of the twenty-first century (2025–2100) compared to the historical reference period (1981–2016). The greatest projected reduction is observed in the SSP3-7.0 - ACCESS-CM2 Figure 7 model, with a loss of more than 370 Mm³, reflecting a serious impact on water resources in this highly forcing scenario. Likewise, under the SSP1-2.6 - ACCESS-CM2 Table 8 scenario, the reduction also exceeds 360 Mm³, indicating that even under sustainable scenarios, the pressure on the water system will persist.

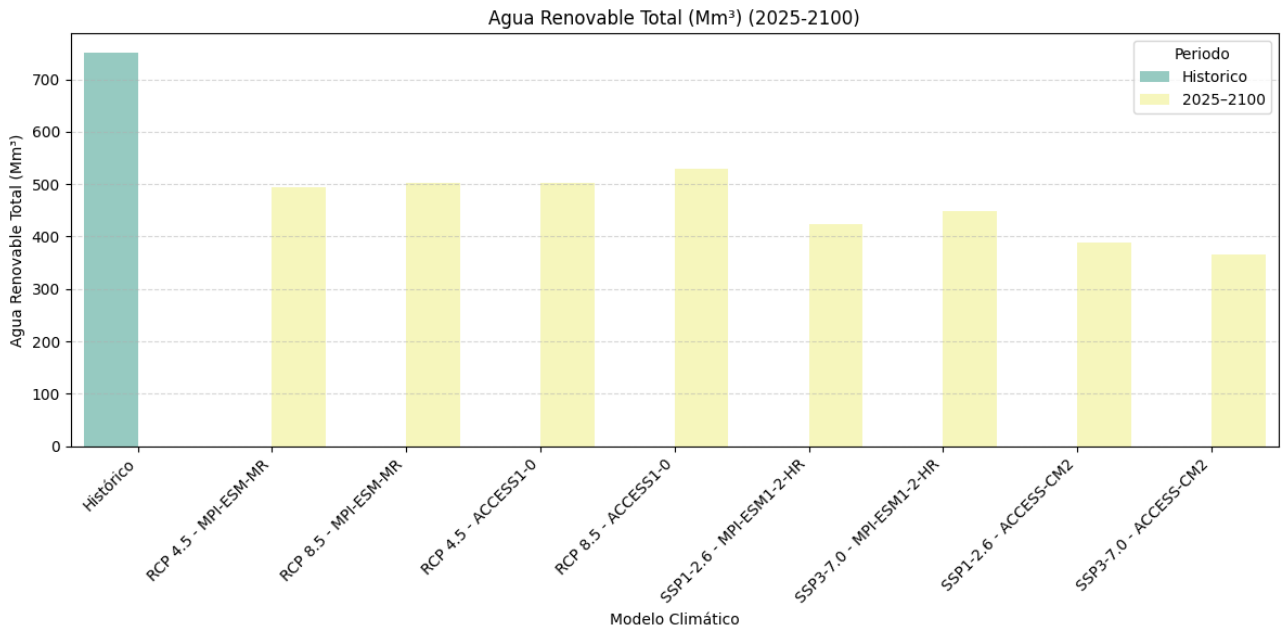

Figure 7. Simulation of renewable water under the climate scenarios examined

On the other hand, models such as RCP 4.5 - MPI-ESM-MR and RCP 4.5 - ACCESS1-0 show moderate reductions of around 220–240 Mm³, although they maintain a better performance in terms of water resilience. In all cases, the comparison shows that, over the next eight decades, renewable resources could be reduced by between 25% and 50%, depending on the model and the climate scenario, which would have direct consequences on the availability of water for human consumption, agriculture and ecosystems.

These findings reinforce the need to implement water adaptation measures and integrated resource management in the region evaluated, anticipating the adverse effects of climate change on the hydrological cycle.

Table 8. Simulation of renewable water under the climate scenarios examined.

Model	Scenario	Period	Renewable Water (Mm^3)
	Base		750.2521812
MPI_ESM_MR	RCP 4.5	2025–2100	494.6925056
MPI_ESM_MR	RCP 8.5	2025–2100	503.5839936
ACCESS1_0	RCP 4.5	2025–2100	502.8694664
ACCESS1_0	RCP 8.5	2025–2100	530.03123087
MPI-ESM1_2_HR	SSP1-2.6	2025–2100	424.2332702
MPI-ESM1_2_HR	SSP3-7.0	2025–2100	449.1450048
ACCESS_CM2	SSP1-2.6	2025–2100	389.4019802
ACCESS_CM2	SSP3-7.0	2025–2100	366.0784793

3.6. Drought severity

One of the main effects of climate change on the hydrological cycle is the appearance of extreme phenomena such as droughts. To evaluate its magnitude and impact on the analyzed basin, the standardized precipitation index (SPI) on an annual scale (SPI-12) was estimated for the period 1981–2016. SPI values below 0 were considered to indicate drought conditions, while values above 1 reflect significant wet periods. As can be seen in Figure 8, the interannual behavior of the SPI shows significant variability. Between 1983 and 1985, predominantly wet conditions were recorded, with maximum SPI values close to +2. However, the year 1991 evidenced a severe drought with an SPI of -2.2, followed by a transitory recovery. Subsequently, in 1997, the most extreme drought of the period was recorded with an SPI of -3.4, coinciding with a strong El Niño event, which caused a negative impact on surface and groundwater resources.

On the contrary, 1996 was a particularly wet year, with an SPI above +2.5, the highest value in the series. From 2008 onwards, a new phase of recurrent drought was observed, highlighting the years 2010, 2014 and 2016, where the SPI remained below -1.5. In particular, 2016 closed with an SPI of -2.1, which represents a severe drought at the end of the period evaluated. In summary, the results show a trend towards intensification and frequency of dry events in the last two decades, which could be associated with changes in regional weather patterns and a decrease in water availability in the basin.

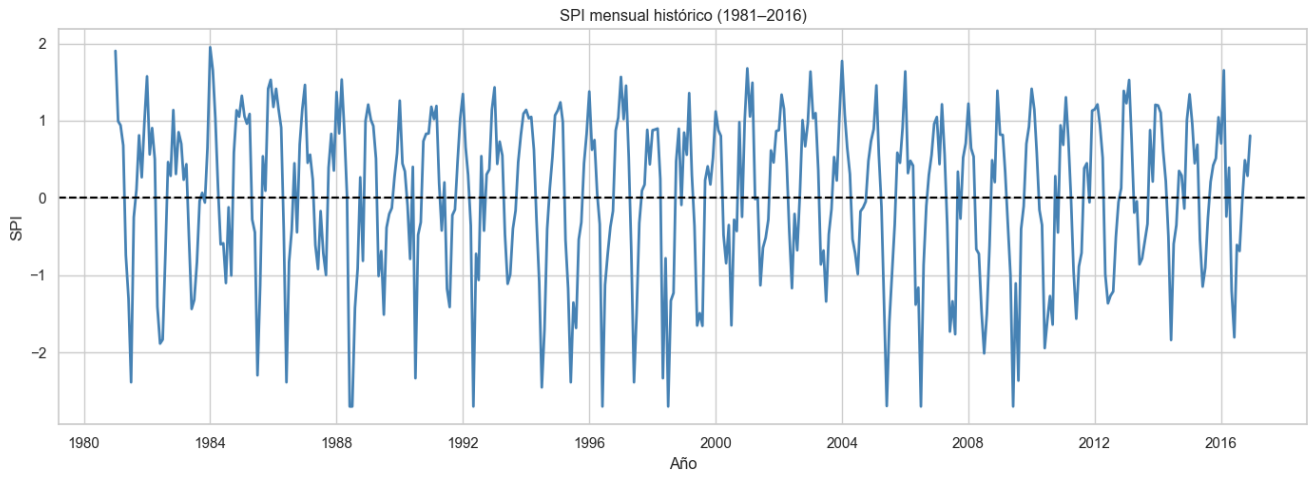

Figure 8. Varamin Plain Standard Precipitation Index (SPI) Graph (1981–2016)

One of the expected effects of climate change in the Peruvian Altiplano is the increase in the frequency and intensity of droughts. To evaluate this phenomenon, the monthly Standardized Precipitation Index (SPI) for the period 2017–2050 was estimated, considering the MPI_ESM_MR and ACCESS models (in their different versions) under the RCP 4.5, RCP 8.5, SSP1-2.6 and SSP3-7.0 scenarios. Figure 9 Projected SPI shows a clear trend towards climate variability with alternating phases of humidity and drought. Under scenario MPI_ESM_MR - RCP 8.5, a marked drought is identified in the year 2028, where the monthly SPI drops below -2, indicating a severe drought. Likewise, the ACCESS1_0 scenario - RCP 8.5 reflects a prolonged decrease in the SPI between 2034 and 2037, reaching critical values close to -2.5. Similarly, in the SSP3-7.0 scenario with the ACCESS_CM2 model, the years 2041 and 2047 present extreme drought indices, which suggests an intensification of future water stress.

The highest projected drought severity is presented in scenario MPI_ESM1_2_HR - SSP3-7.0 during the year 2043, where the SPI falls below -2.8. This event could have substantial impacts on water recharge, agriculture, and ecosystems in the region, exacerbating challenges to sustainable water management. The evaluation of the number of dry years and their frequency reveals a greater recurrence of extreme events compared to the historical period, which reinforces the need to implement climate adaptation strategies and advance planning in the use of water resources.

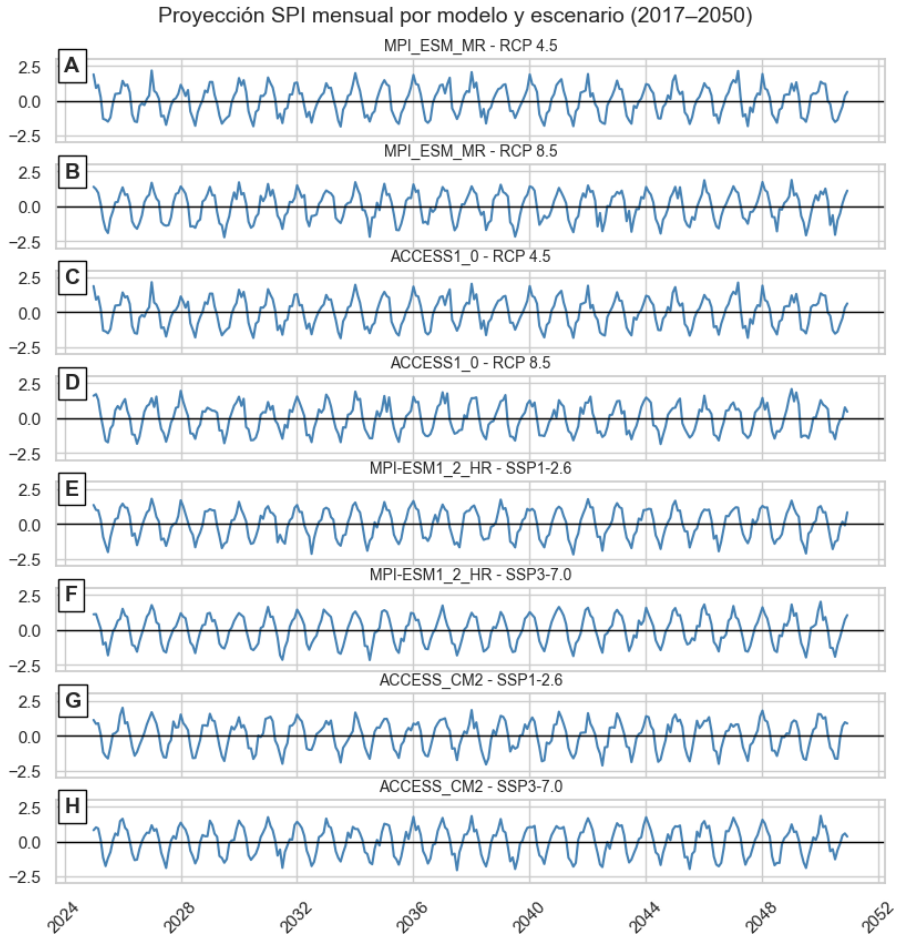

Figure 9. The SPI index for the period 2017–2050 under RCP and SSP climate scenarios (2017–2050)

4. Discussions

The results obtained by applying the SWAT hydrological model in the Huancané River basin provide a detailed view of how climate change could affect water resources in this region. Significant variability in surface runoff was observed under different emission scenarios. Specifically, the CMIP5 RCP 8.5 and RCP 4.5 scenarios indicate increases in runoff, while the CMIP6 SSP1-2.6 and SSP3-7.0 scenarios project a progressive decrease towards the end of the century. This disparity suggests that the severity of climate change and its impact on the hydrological cycle depend on both radiative forcing and underlying socioeconomic assumptions. The dynamics of the observed runoff respond mainly to two factors: the projected increase in temperature and the variability

in precipitation. In the most extreme scenarios, the thermal increase increases potential evapotranspiration, reducing the volume of water available for runoff and groundwater recharge. This result is consistent with previous studies in the Andes, where it has been documented that temperature increase has a more pronounced effect on water availability than variation in precipitation, due to the intensification of water stress in soils and lower infiltration efficiency[48]. In relation to groundwater recharge, the data show a significant reduction in all scenarios, with RCP 8.5 being the most critical. This finding is of great relevance, as it confirms the vulnerability of aquifers to climate change. Lower infiltration and percolation rates could lead to a lower availability of groundwater for agricultural and domestic use, which seriously compromises water security in rural areas of the Puno region. Previous research has warned that this type of impact is aggravated in basins with a predominance of baseflow and low surface runoff, conditions present in Huancané[47].

On the other hand, the analysis of the volume of renewable water reveals a generalized trend of decline towards the year 2100. This reduction exceeds 50% in the SSP3-7.0 scenario, which represents an alert about the possible adverse effects on the sustainability of ecosystems and the management of water demand. Although some moderate scenarios such as RCP 4.5 show less severe reductions, even in these cases the cumulative impact on the hydrological cycle will be considerable. The combination of water stress, population pressure and increased agricultural demand poses complex challenges for local and regional water planning authorities[49].The analysis of drought using the SPI index further reinforces this picture. The historical results show an intensification of droughts in recent decades, with severe events recorded in 1997 and 2016. Projections for the period 2025–2050 under RCP and SSP scenarios show a higher frequency and intensity of dry events, especially in the years 2028, 2034–2037 and 2043. This pattern of recurrent droughts poses a critical threat to subsistence agriculture, aquifer recharge, and the maintenance of minimal ecological flows [50].

In comparative terms, the CMIP6 models offer more conservative projections than those of CMIP5. However, the SSP3-7.0 scenario that assumes high emissions, accelerated population growth and low international cooperation turns out to be the most alarming in terms of water stress. On the other hand, the SSP1-2.6 scenario, associated with sustainable policies and a transition to clean energy, presents better projections, although it still shows signs of reduction in renewable and groundwater[51]. These results are in line with what was reported by the IPCC, which highlights that the impacts of climate change on water resources are highly sensitive to the type of socioeconomic trajectory adopted at the global and regional levels [8]. The usefulness of the SWAT model was evidenced not only in the ability to simulate complex hydrological processes with scarce data, but also in its adaptability to incorporate corrected climate projections. The combined use of satellite data, bias correction tools and automatic calibration allowed to obtain robust simulations, validated with R^2 coefficients greater than 0.80. This level of accuracy is comparable to that of similar investigations in basins of the Ecuadorian and Colombian Andes [52].

Climate projections carry a high degree of uncertainty due to variability among Global Climate Models (GCMs), the range of emission scenarios (such as RCPs or SSPs), downscaling methods, and natural climate variability. These sources of uncertainty are especially relevant in mountainous regions like the Huancané River basin, where complex topography and limited data availability hinder the accuracy of estimates. GCMs differ in how they simulate key processes such as precipitation and temperature, while downscaling can introduce additional biases. Furthermore, phenomena like the El Niño–Southern Oscillation (ENSO) generate interannual fluctuations that may obscure long-term trends projected by climate models.

On the other hand, hydrological models used to assess the impacts of climate change also incorporate simplified assumptions that affect their predictive capacity. Most of these models assume stationary relationships between climatic and hydrological variables, overlooking possible changes in system responses under new climate conditions. Parameter calibration using historical data—often scarce or imprecise in the Andes—introduces further uncertainty. Additionally, key factors such as glacier retreat and land use change are not always dynamically integrated. Therefore, it is recommended to use ensemble modeling approaches, sensitivity analyses, and uncertainty quantification methods to provide more robust projections that support sustainable water management in the Huancané River basin.

5. Conclusions

Climate change in surface runoff, percolation, aquifer recharge and renewable water resources in the Huancané basin of the Peruvian Andean highlands, during the period 2025–2050, using the SWAT hydrological model and projections of the RCP 4.5, RCP 8.5, SSP1-2.6 and SSP3-7.0 climate scenarios. The results showed that under severe scenarios such as SSP3-7.0, surface runoff will decrease considerably, reaching only 8.09 m^3/s,

compared to the 12.59 m³/s projected in RCP 8.5. The recharge of aquifers, which in the base period was 559.22 Mm³, will fall to 179.09 Mm³, and the volume of renewable water will be reduced by 51.2%, from 750 Mm³ to 366 Mm³. In addition, the average annual temperature in the basin is projected to reach 14 °C by the end of the 21st century, intensifying evapotranspiration processes and reducing water availability. The analysis of the SPI index reveals a trend towards more frequent and severe droughts during the period 2025–2050 in all the scenarios evaluated. These results show that the thermal increase and the decrease in precipitation will be determining factors in the reduction of surface and groundwater resources. The SWAT model proved to be an effective tool for estimating these impacts, generating useful inputs for adaptive planning. If water adaptation measures, such as reforestation, storage, irrigation efficiency, and institutional strengthening, are not implemented, the sustainability of water resources in the Huancané basin could be seriously compromised by the end of the century. This knowledge must be integrated into water management decisions in high Andean regions vulnerable to climate change.

To enhance resilience to the projected hydrological impacts of climate change in the Huancané River basin, water management strategies must incorporate both socioeconomic factors and land use changes. Rapid population growth, agricultural intensification, and increasing water demand can intensify pressure on already stressed water systems, particularly during prolonged droughts. Additionally, land use changes such as deforestation, overgrazing, and urban expansion can reduce infiltration, degrade watersheds, and alter natural hydrological responses. Adaptive measures should include decentralized water storage infrastructure, efficient irrigation technologies, sustainable land use planning, and the integration of climate indicators like the SPI into early warning systems. Strengthening local water governance, enhancing hydrometeorological monitoring, and involving local communities in decision-making processes are also key to ensuring equitable and sustainable water use in a changing climate.

To enhance resilience against the projected hydrological impacts of climate change, it is essential to implement adaptive water management strategies in the Huancané River basin. These should include the development of decentralized water storage systems to buffer seasonal shortages, the promotion of efficient irrigation technologies to reduce water losses, and the integration of climate data—such as SPI-based drought forecasts—into early warning and decision-making systems. Strengthening local water governance, investing in hydrometeorological monitoring networks, and incorporating community-based adaptation approaches can further support sustainable water use. Additionally, long-term planning must consider glacier retreat and shifting precipitation patterns to ensure equitable and reliable water supply for all sectors.

Declaration of competing interest

The authors declare that they have no any known financial or non-financial competing interests in any material discussed in this paper.

Funding information

No funding was received from any financial organization to conduct this research.

Author contribution

The contribution to the paper is as follows: J. Hinojosa, A, Mamani, J. Apaza: study conception and design; J. Apaza, L. Quea, N, Villanueva: data collection; A, Calderon, V. Alanoca, Y, Maquera: analysis and interpretation of results; S. Cotrado, S. Zegarra, J. Inquilla: draft preparation. All authors approved the final version of the manuscript.

References

[1] E. Foroumandi, V. Nourani, and E. Sharghi, “Climate change or regional human impacts? Remote sensing tools, artificial neural networks, and wavelet approaches aim to solve the problem,” *Hydrol. Res.*, vol. 52, no. 1, pp. 176–195, 2021, https://doi: 10.2166/NH.2020.112.

[2] S. Karam, B. S. Zango, O. Seidou, D. Perera, N. Nagabhatla, and R. M. Tshimanga, “Impacts of Climate Change on Hydrological Regimes in the Congo River Basin,” *Sustain.*, vol. 15, no. 7, pp. 1–19, 2023, https://doi: 10.3390/su15076066.

[3] G. Dharmarathne, A. O. Waduge, M. Bogahawaththa, U. Rathnayake, and D. P. P. Meddage, “Adapting cities to the surge: A comprehensive review of climate-induced urban flooding,” *Results Eng.*, vol. 22, no. April, p. 102123, 2024, https://doi: 10.1016/j.rineng.2024.102123.

[4] Z. Kalantari, C. S. S. Ferreira, R. P. D. Walsh, A. J. D. Ferreira, and G. Destouni, "Urbanization Development under Climate Change: Hydrological Responses in a Peri-Urban Mediterranean Catchment," *L. Degrad. Dev.*, vol. 28, no. 7, pp. 2207–2221, 2017, https://doi: 10.1002/ldr.2747.

[5] F. Asurza, C. Ramos, and W. Lavado, "Assessment of Tropical Rainfall Measuring Mission (TRMM) and Global Precipitation Measurement (GPM) products in hydrological modeling of the Huancane river basin, Peru," *Sci. Agropecu.*, vol. 9, no. 1, pp. 53–62, 2018, https://doi: 10.17268/sci.agropecu.2018.01.06.

[6] G. Huaccoto and H. Calderon, "Determinación del método eficiente para calcular la evapotranspiración potencial para un modelo Lluvia - escorrentía en la cuenca Huancané Puno Determination," *Aporte Santiaguino*, vol. 12, no. 2, pp. 214–227, 2020.

[7] R. G. Patricia, M. R. A. Ismael, A. C. Conde Álvarez, and G. S. Torres Esqueda, "Breve Guía para la Selección, Descarga y Aplicación de Escenarios de Cambio Climático para México. De acuerdo con los últimos escenarios del IPCC," 2022. https://doi: 10.13140/RG.2.2.20064.15369.

[8] Senamhi, "Evaluación de los modelos CMIP5 del IPCC en el," vol. 6141414, 2013.

[9] J. Janjić and L. Tadić, "Fields of Application of SWAT Hydrological Model—A Review," *Earth (Switzerland)*, vol. 4, no. 2, pp. 331–344, 2023, https://doi: 10.3390/earth4020018.

[10] S. Aloui, A. Mazzoni, A. Elomri, J. Aouissi, A. Boufekane, and A. Zghibi, "A review of Soil and Water Assessment Tool (SWAT) studies of Mediterranean catchments: Applications, feasibility, and future directions," *J. Environ. Manage.*, vol. 326, no. PB, p. 116799, 2023, https://doi: 10.1016/j.jenvman.2022.116799.

[11] L. T. Ha, W. G. M. Bastiaanssen, A. van Griensven, A. I. J. M. van Dijk, and G. B. Senay, "Calibration of spatially distributed hydrological processes and model parameters in SWAT using remote sensing data and an auto-calibration procedure: A case study in a Vietnamese river basin," *Water (Switzerland)*, vol. 10, no. 2, 2018, https://doi: 10.3390/w10020212.

[12] P. T. Hlaing, U. W. Humphries, and M. Waqas, "Hydrological model parameter regionalization: Runoff estimation using machine learning techniques in the Tha Chin River Basin, Thailand," *MethodsX*, vol. 13, no. April, p. 102792, 2024, https://doi: 10.1016/j.mex.2024.102792.

[13] S. Haider *et al.*, "Simulation of the Potential Impacts of Projected Climate and Land Use Change on Runoff under CMIP6 Scenarios," *Water (Switzerland)*, vol. 15, no. 19, 2023, doi: 10.3390/w15193421.

[14] M. J. Hayes, M. D. Svoboda, D. A. Wilhite, and O. V. Vanyarkho, "Monitoring the 1996 Drought Using the Standardized Precipitation Index," *Bull. Am. Meteorol. Soc.*, vol. 80, no. 3, pp. 429–438, 1999, https://doi: 10.1175/1520-0477(1999)080<0429:MTDUTS>2.0.CO;2.

[15] T. Iwata *et al.*, "Preoperative serum value of sialyl Lewis X predicts pathological nodal extension and survival in patients with surgically treated small cell lung cancer," *J. Surg. Oncol.*, vol. 105, no. 8, pp. 818–824, 2012, https://doi: 10.1002/jso.23002.

[16] M. N. Lorenzo, H. Pereira, I. Alvarez, and J. M. Dias, "Standardized Precipitation Index (SPI) evolution over the Iberian Peninsula during the 21st century," *Atmos. Res.*, vol. 297, no. November 2023, p. 107132, 2024, https://doi: 10.1016/j.atmosres.2023.107132.

[17] J. Spinoni, G. Naumann, J. V. Vogt, and P. Barbosa, "The biggest drought events in Europe from 1950 to 2012," *J. Hydrol. Reg. Stud.*, vol. 3, pp. 509–524, 2015, https://doi: 10.1016/j.ejrh.2015.01.001.

[18] M. Hayes, M. Svoboda, N. Wall, and M. Widhalm, "The lincoln declaration on drought indices: Universal meteorological drought index recommended," *Bull. Am. Meteorol. Soc.*, vol. 92, no. 4, pp. 485–488, 2011, https://doi: 10.1175/2010BAMS3103.1.

[19] S. Marahatta, D. Aryal, L. P. Devkota, U. Bhattarai, and D. Shrestha, "Application of swat in hydrological simulation of complex mountainous river basin (Part ii: Climate change impact assessment)," *Water (Switzerland)*, vol. 13, no. 11, 2021, https://doi: 10.3390/w13111548.

[20] J. A. Quiroz *et al.*, "Water Resources Evaluation and Sustainability Considering Climate Change and Future Anthropic Demands in the Arequipa Region of Southern Peru," *Sustain.*, vol. 15, no. 23, 2023,

https://doi: 10.3390/su152316270.

[21] R. F. P. Murillo, W. Lavado Casimiro, Y. C. Pachac Huerta, M. Zapana Quispe, and D. Guevara-Freire, "Using the SWAT Model to Simulate the Hydrological Response to LULC in a Binational Basin between Ecuador and Peru," *Eng. Technol. Appl. Sci. Res.*, vol. 14, no. 6, pp. 17816–17823, 2024, https://doi: 10.48084/etasr.8646.

[22] S. Khalilian and N. Shahvari, "A SWAT Evaluation of the Effects of Climate Change on Renewable Water Resources in Salt Lake Sub-Basin, Iran," *AgriEngineering*, vol. 1, no. 1, pp. 44–57, 2019, https://doi: 10.3390/agriengineering1010004.

[23] S. Vanaja, "Acceso a agua corriente, ahorro de tiempo y ausentismo escolar: evidencia de la India," *AgEcon Search*, 2018.

[24] C. Tancayllo, "Gobernanza hídrica para la disponibilidad de agua en áreas de influencia minera caso: comunidad de Alto Huarca de la provincia de Espinar - Perú," 2021. [Online]. Available: https://educacion.gob.ec/wp-content/uploads/downloads/2021/02/Pasa-la-Voz-Enero-2021.pdf

[25] L. Hinojosa, "Elementos para el debate sobre la gobernanza ambiental en los Andes, con especial mención al agua y minería en el Perú," *Rev. Cienc. Política*, vol. 6, no. 4, pp. 33–45, 2013.

[26] P. A. Jiménez Cabrera, M. Hernández Juárez, G. Espinosa Sánchez, G. Mendoza Castelán, and M. B. Torrijos Almazán, "Los saberes en medicina tradicional y su contribución al desarrollo rural: estudio de caso Región Totonaca, Veracruz," *Rev. Mex. Ciencias Agrícolas*, vol. 6, no. 8, pp. 1791–1805, 2017, https://doi: 10.29312/remexca.v6i8.496.

[27] D. Urbina and M. Quispe, "La pobreza monetaria desde la perspectiva de la pobreza multidimensional: el caso peruano," *Enfoque*, vol. 4, no. 2–3, pp. 77–98, 2016, https://doi: 10.26439/enfoque2016.n002.1871.

[28] S. Naish, P. Dale, J. S. Mackenzie, J. McBride, K. Mengersen, and S. Tong, "Climate change and dengue: A critical and systematic review of quantitative modelling approaches," *BMC Infect. Dis.*, vol. 14, no. 1, 2014, https://doi: 10.1186/1471-2334-14-167.

[29] K. Solaun and E. Cerdá, "Climate change impacts on renewable energy generation. A review of quantitative projections," *Renew. Sustain. Energy Rev.*, vol. 116, 2019, https://doi: 10.1016/j.rser.2019.109415.

[30] N. Schaller, I. Mahlstein, J. Cermak, and R. Knutti, "Analyzing precipitation projections: A comparison of different approaches to climate model evaluation," *J. Geophys. Res. Atmos.*, vol. 116, no. 10, pp. 1–14, 2011, https://doi: 10.1029/2010JD014963.

[31] M. D. Webster and A. P. Sokolov, "A methodology for quantifying uncertainty in climate projections," *Clim. Change*, vol. 46, no. 4, pp. 417–446, 2000, https://doi: 10.1023/A:1005685317358.

[32] C. Alvar *et al.*, "Uso del Producto Grillado PISCO de precipitación en Estudios, Investigaciones y Sistemas Operacionales de Monitoreo y Pronóstico Hidrometeorológico," 2017.

[33] J. G. Arnold, R. Srinivasan, R. S. Muttiah, and J. R. Williams, "Large area hydrologic modeling and assessment part I: Model development," *Journal of the American Water Resources Association*, vol. 34, no. 1. pp. 73–89, 1998. https://doi: 10.1111/j.1752-1688.1998.tb05961.x.

[34] M. K. Rowshon, N. S. Dlamini, M. A. Mojid, M. N. M. Adib, M. S. M. Amin, and S. H. Lai, "Modeling climate-smart decision support system (CSDSS) for analyzing water demand of a large-scale rice irrigation scheme," *Agric. Water Manag.*, vol. 216, pp. 138–152, 2019, https://doi: 10.1016/j.agwat.2019.01.002.

[35] C. Oeurng, T. A. Cochrane, M. E. Arias, B. Shrestha, and T. Piman, "Assessment of changes in riverine nitrate in the Sesan, Srepok and Sekong tributaries of the Lower Mekong River Basin," *J. Hydrol. Reg. Stud.*, vol. 8, pp. 95–111, 2016, https://doi: 10.1016/j.ejrh.2016.07.004.

[36] A. K. Basheer, H. Lu, A. Omer, A. B. Ali, and A. M. S. Abdelgader, "Impacts of climate change under CMIP5 RCP scenarios on the streamflow in the Dinder River and ecosystem habitats in Dinder National Park, Sudan," *Hydrol. Earth Syst. Sci.*, vol. 20, no. 4, pp. 1331–1353, 2016, https://doi: 10.5194/hess-

20-1331-2016.

[37] M. Iqbal, J. Wen, M. Masood, M. U. Masood, and M. Adnan, "Impacts of Climate and Land-Use Changes on Hydrological Processes of the Source Region of Yellow River, China," *Sustain.*, vol. 14, no. 22, pp. 1–21, 2022, https://doi: 10.3390/su142214908.

[38] A. Anandhi *et al.*, "Examination of change factor methodologies for climate change impact assessment," *Water Resour. Res.*, vol. 47, no. 3, pp. 1–10, 2011, https://doi: 10.1029/2010WR009104.

[39] M. Winchell, R. Srinivasan, M. Di Luzio, and J. Arnold, "ArcSWAT interface for SWAT2009 User's Guide," *User's Guid.*, p. 489, 2010.

[40] C. Santhi, N. Kannan, J. G. Arnold, and M. Di Luzio, "Spatial calibration and temporal validation of flow for regional scale hydrologic modeling," *J. Am. Water Resour. Assoc.*, vol. 44, no. 4, pp. 829–846, 2008, https://doi: 10.1111/j.1752-1688.2008.00207.x.

[41] A. G. Mengistu, L. D. van Rensburg, and Y. E. Woyessa, "Techniques for calibration and validation of SWAT model in data scarce arid and semi-arid catchments in South Africa," *J. Hydrol. Reg. Stud.*, vol. 25, no. August, p. 100621, 2019, https://doi: 10.1016/j.ejrh.2019.100621.

[42] A. Bennour *et al.*, "Calibration and Validation of SWAT Model by Using Hydrological Remote Sensing Observables in the Lake Chad Basin," *Remote Sens.*, vol. 14, no. 6, 2022, https://doi: 10.3390/rs14061511.

[43] K. C. Abbaspour, "SWAT-COPA 2012. Programa de Calibración e Incertidumbre SWAT—A Manual del usuario," 2012.

[44] E. Servat and A. Dezetter, "Sélection de fonctions critères dans le cadre d%une modélisation pluie-débit en zone de savane soudanaise," *Hydrol. Sci. J.*, vol. 36, no. 4, pp. 307–330, 1991, https://doi: 10.1080/02626669109492517.

[45] M. Geza, K. E. Murray, and J. E. McCray, "Watershed-Scale Impacts of Nitrogen from On-Site Wastewater Systems: Parameter Sensitivity and Model Calibration," *J. Environ. Eng.*, vol. 136, no. 9, pp. 926–938, 2010, https://doi: 10.1061/(asce)ee.1943-7870.0000232.

[46] S. J. Maeng, M. Azam, H. S. Kim, and J. H. Hwang, "Analysis of changes in spatio-temporal patterns of drought across South Korea," *Water (Switzerland)*, vol. 9, no. 9, pp. 1–20, 2017, https://doi: 10.3390/w9090679.

[47] C. Liu, C. Yang, Q. Yang, and J. Wang, "Spatiotemporal drought analysis by the standardized precipitation index (SPI) and standardized precipitation evapotranspiration index (SPEI) in Sichuan Province, China," *Sci. Rep.*, vol. 11, no. 1, pp. 1–14, 2021, https://doi: 10.1038/s41598-020-80527-3.

[48] W. Buytaert, M. Vuille, A. Dewulf, R. Urrutia, A. Karmalkar, and R. Célleri, "Uncertainties in climate change projections and regional downscaling in the tropical Andes: Implications for water resources management," *Hydrol. Earth Syst. Sci.*, vol. 14, no. 7, pp. 1247–1258, 2010, https://doi: 10.5194/hess-14-1247-2010.

[49] D. E. Barra-Quispe *et al.*, "Economic, Social, Cultural Capital of the Region of Puno, Peru," *J. Ecohumanism*, vol. 3, no. 7, pp. 1207–1229, 2024, https://doi: 10.62754/joe.v3i7.4280.

[50] V. A. Ángeles Clemente, D. P. R. Arana Ruedas, S. D. Camargo Hinostroza, and O. Oketta, "Comparison between Standardized Precipitation Index (SPI) and Standardized Evapotranspiration Index (SPEI) for agricultural drought over Mantaro Valley, Peru," *Manglar*, vol. 21, no. 3, pp. 337–345, 2024, https://doi: 10.57188/manglar.2024.037.

[51] A. Mamani-Flores, J. R. Romero-Cahuana, O. Choquehuanca-Tintaya, V. Málaga-Apaza, and E. A. Chambi-Idme, "Mechanisms for citizen participation during the national crisis process: citizens speak," *Rev. Bras. Políticas Públicas*, vol. 14, no. 1, pp. 283–295, 2024, doi: https://doi.org/10.5102/rbpp.v14i3.9136.

[52] F. X. Jarrin-Perez *et al.*, "SWAT Simulation of a Small Neotropical Alpine Catchment in the Ecuadorian Andes," *ESSOAr*, no. May, 2022, https://doi: 10.1002/essoar.10511242.1.